Electronic Supplementary Material (ESI) for ChemComm.

A novel fluorescent probe for paraquat and cyanide in water based on pillar[5]arene/10-methylacridinium iodide molecular recognition

Pi Wang, Yong Yao and Min Xue*

Department of Chemistry, Zhejiang University, Hangzhou 310027, P. R. China;

Fax and Tel: +86-571-8795-3189; Email address: xuemin@zju.edu.cn.

Electronic Supplementary Information (ESI)

1. Materials and methods

All reagents were commercially available and used as supplied without further purification. Compounds **WP5**[S1] and **G**[S2] were prepared according to the published procedures. NMR spectra were recorded with a Bruker Avance DMX 500 spectrophotometer or a Bruker Avance DMX 400 spectrophotometer using the deuterated solvent as the lock and the residual solvent or TMS as the internal reference. Low-resolution electrospray ionization mass spectra were recorded with a Bruker Esquire 3000 Plus spectrometer. High-resolution mass spectrometry experiments were performed with a Bruker Daltonics Apex III spectrometer. 2D ^{1}H-^{1}H NOESY spectrum was collected on a Bruker Advance DMX-500 spectrometer. Mass spectra were obtained on a Bruker Esquire 3000 plus mass spectrometer (Bruker-Franzen Analytik GmbH Bremen, Germany) equipped with an ESI interface and an ion trap analyzer. UV-vis spectra were taken on a Shimadzu UV-2550 UV-vis spectrophotometer. The fluorescence experiments were conducted on a RF-5301 spectrofluorophotometer (Shimadzu Corporation, Japan). Isothermal titration calorimetric (ITC) measurements were performed on a VP-ITC micro-calorimeter (Microcal, USA). HRMS were obtained on a Bruker 7-Tesla FT-ICRMS equipped with an electrospray source (Billerica, MA, USA). The melting points were collected on a SHPSIC WRS-2 automatic melting point apparatus.

*2. Proton NMR spectra of **G** and **WP5***

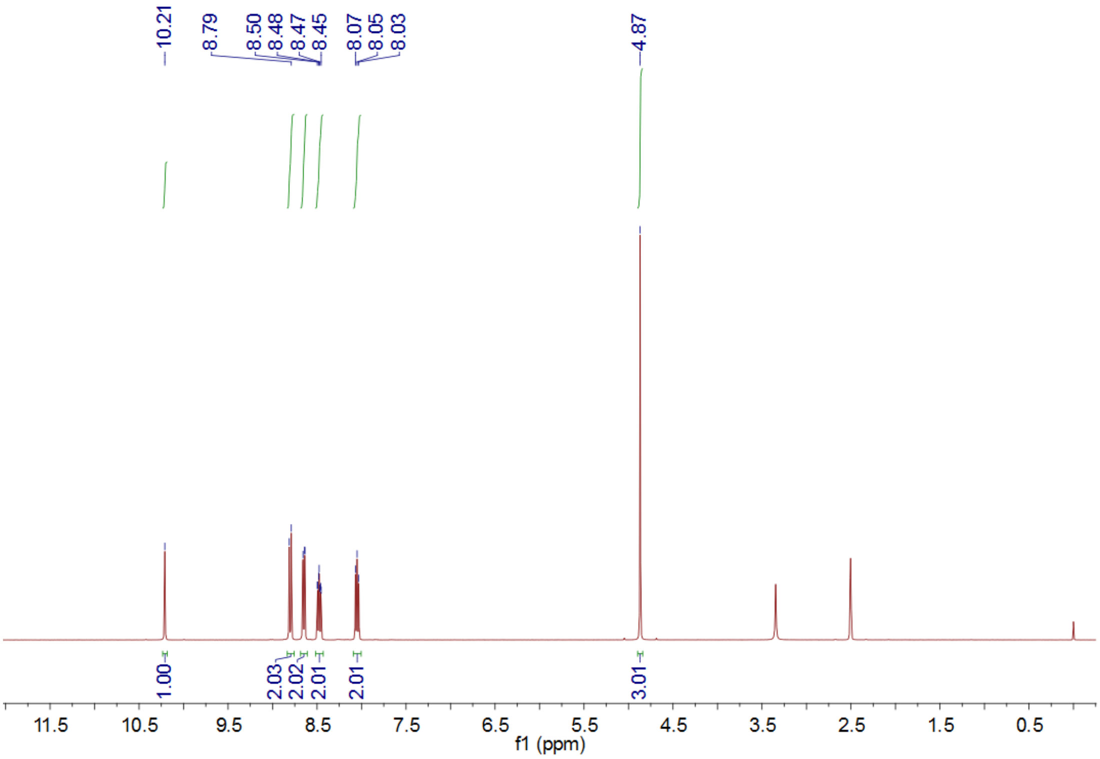

Figure S1. ^{1}H NMR spectrum (400 Hz, DMSO-d_6, 298 K) of **G**.

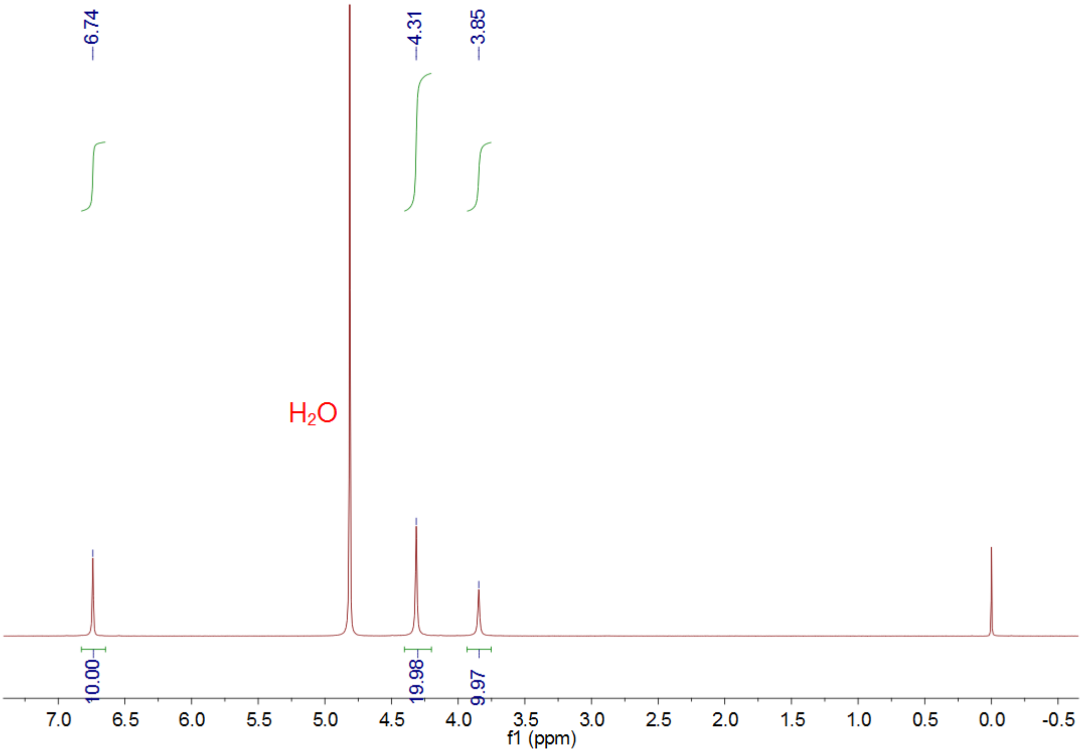

Figure S2. ^{1}H NMR spectrum (400 Hz, D_2O, 298 K) of **WP5**.

3. NOESY NMR spectrum of ***WP5⊐G*** *in* D_2O

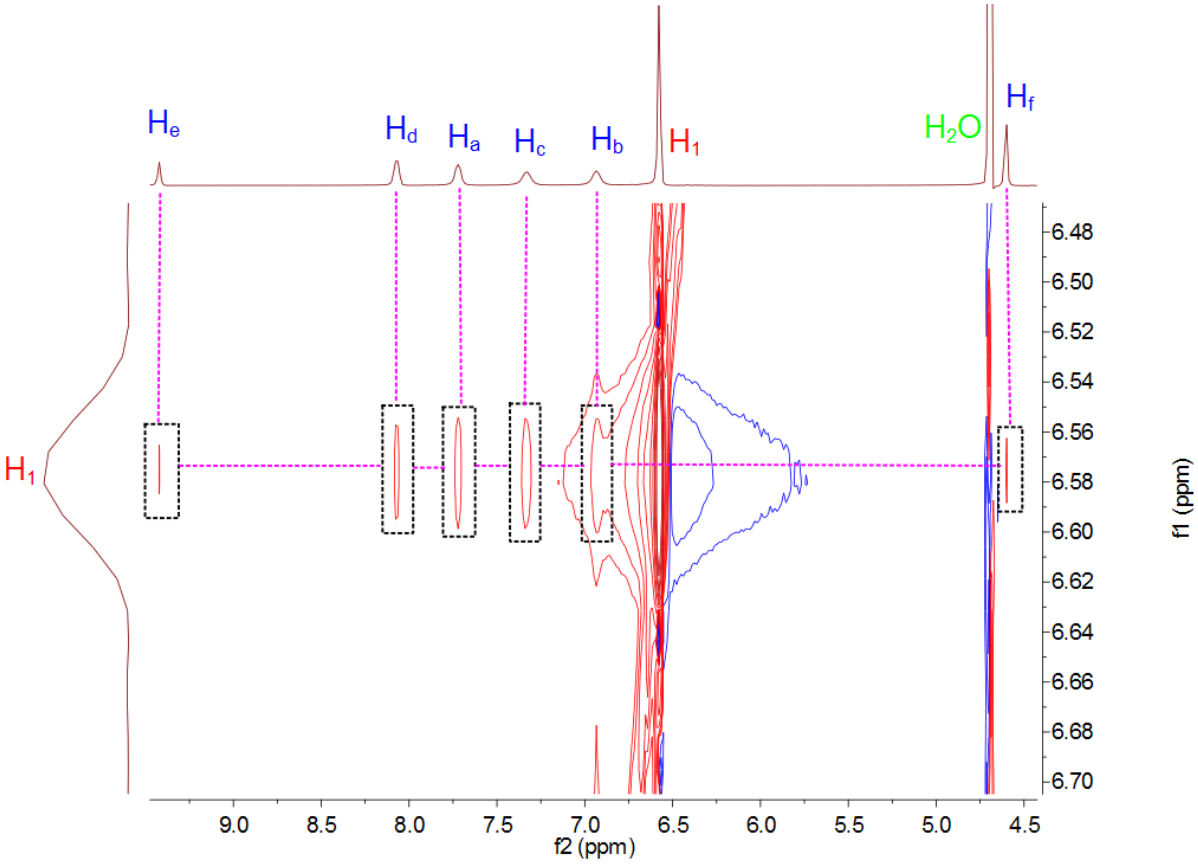

Figure S3. Partial NOESY NMR spectrum (500 MHz, D_2O, 298 K) of 10.0 mM **WP5** and **G**.

4. Stoichiometry and association constant determination for ***WP5⊐G*** *and* ***WP5***⊐*paraquat in* H_2O

To determine the stoichiometries and association constants of **WP5⊐G** and **WP5**⊐paraquat, ^{1}H NMR titrations were done. By a non-linear curve-fitting method, the association constants between the guests and hosts were calculated. By a mole ratio plot, the stoichiometries were determinated.

(a) Stoichiometry and association constant determination for ***WP5⊐G*** *in* H_2O

The non-linear curve-fitting was based on the equation:[S3]

$$\Delta\delta = (\Delta_\infty/[\mathbf{WP5}]_0)\ (0.5[\mathbf{G}]_0 + 0.5([\mathbf{WP5}]_0 + 1/K_a) - (0.5\ ([\mathbf{G}]_0^2 + (2[\mathbf{G}]_0(1/K_a - [\mathbf{WP5}]_0)) + (1/K_a + [\mathbf{WP5}]_0)^2)^{0.5}))$$

(Eq. S1)

Where $\Delta\delta$ is the chemical shift change of H_3 on **WP5** at $[\mathbf{G}]_0$, Δ_∞ is the chemical shift change of H_3 when the host is completely complexed, $[\mathbf{WP5}]_0$ is the fixed initial concentration of the host, and $[\mathbf{G}]_0$ is the varying concentration of guest **G**.

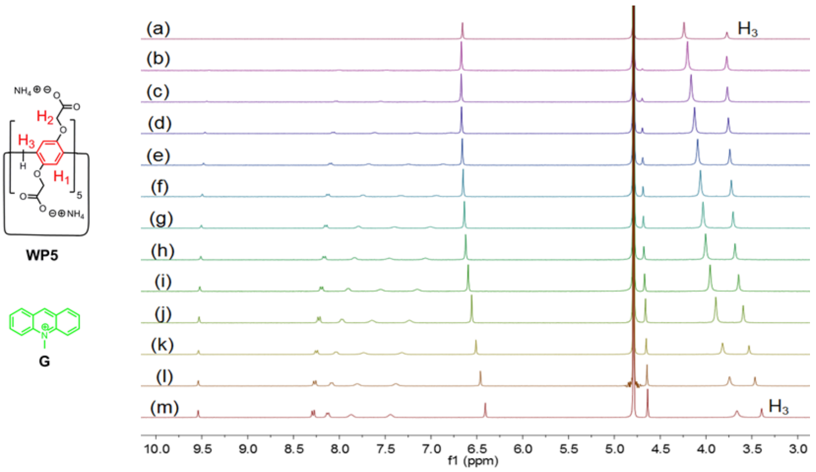

Figure S4. ^{1}H NMR spectra (400 MHz, D_2O, 293 K) of **WP5** at a concentration of 1.00 mM with different concentrations of **G**: (a) 0.00 mM; (b) 0.196 mM; (c) 0.385 mM; (d) 0.566 mM; (e) 0.741 mM; (f) 0.909 mM; (g) 1.07 mM; (h) 1.23 mM; (i) 1.53 mM; (j) 1.94 mM; (k) 2.48 mM; (l) 3.10 mM; (m) 3.94 mM.

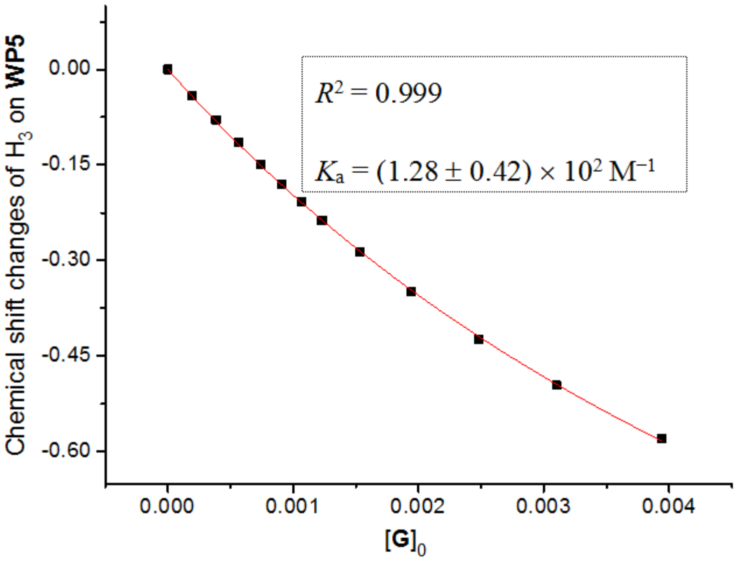

Figure S5. The chemical shift changes of H_3 on **WP5** upon addition of **G**. The red solid line was obtained from the non-linear curve-fitting using Eq. S1.

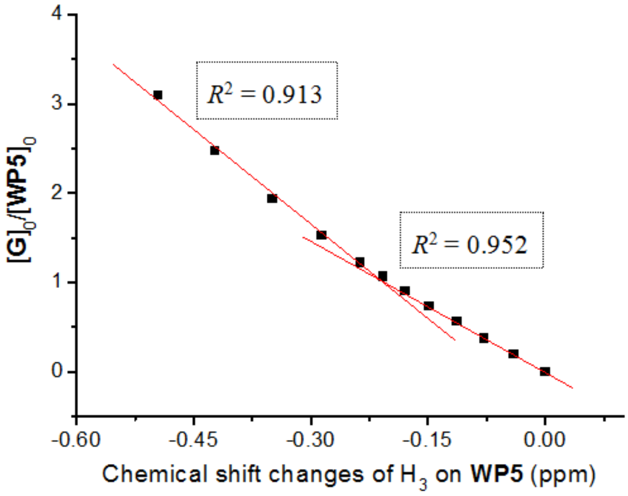

Figure S6. Mole ratio plot for the complexation between **WP5** and **G**, indicating a 1 : 1 stoichiometry.

*(b) Stoichiometry and association constant determination for **WP5**⊃paraquat in H_2O*

$\Delta\delta = (\Delta_\infty/[\text{paraquat}]_0)\ (0.5[\mathbf{WP5}]_0 + 0.5([\text{paraquat}]_0+1/K_a) - (0.5\ ([\mathbf{WP5}]_0^2 + (2[\mathbf{WP5}]_0(1/K_a - [\text{paraquat}]_0)) + (1/K_a + [\text{paraquat}]_0)^2)^{0.5}))$ (Eq. S2)

Where $\Delta\delta$ is the chemical shift change of H_K on paraquat at $[\mathbf{WP5}]_0$, Δ_∞ is the chemical shift change of H_K when the guest is completely complexed, $[\text{paraquat}]_0$ is the fixed initial concentration of the guest, and $[\mathbf{WP5}]_0$ is the varying concentration of host **WP5**.

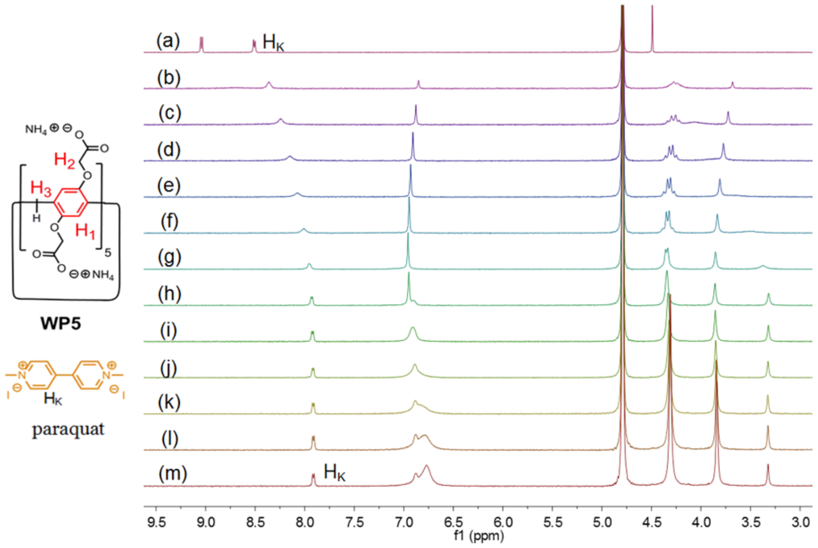

Figure S7. ^{1}H NMR spectra (400 MHz, D_2O, 293 K) of paraquat at a concentration of 1.00 mM with different concentrations of **WP5**: (a) 0.00 mM; (b) 0.196 mM; (c) 0.385 mM; (d) 0.566 mM; (e) 0.741 mM; (f) 0.909 mM; (g) 1.07 mM; (h) 1.23 mM; (i) 1.53 mM; (j) 1.94 mM; (k) 2.48 mM; (l) 3.10 mM; (m) 3.94 mM.

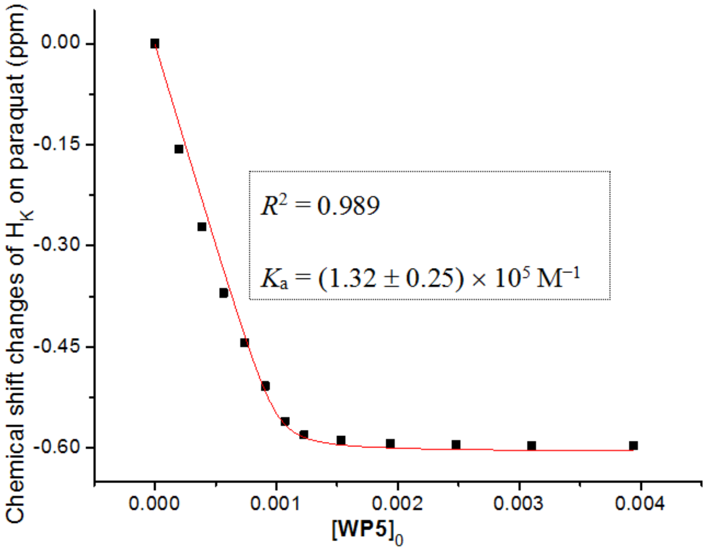

Figure S8. The chemical shift changes of H_K on paraquat upon addition of **WP5**. The red solid line was obtained from the non-linear curve-fitting using Eq. S2.

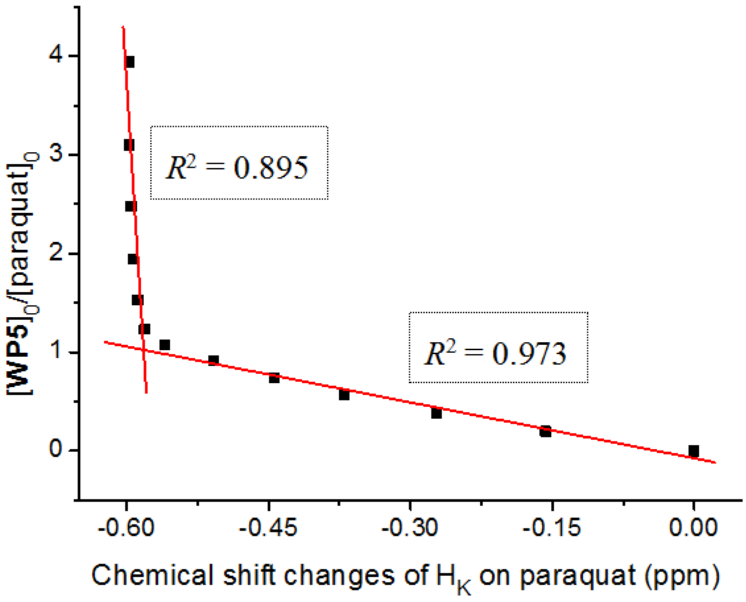

Figure S9. Mole ratio plot for the complexation between **WP5** and paraquat, indicating a 1 : 1 stoichiometry.

*5. UV−vis investigation of **WP5⊃G***

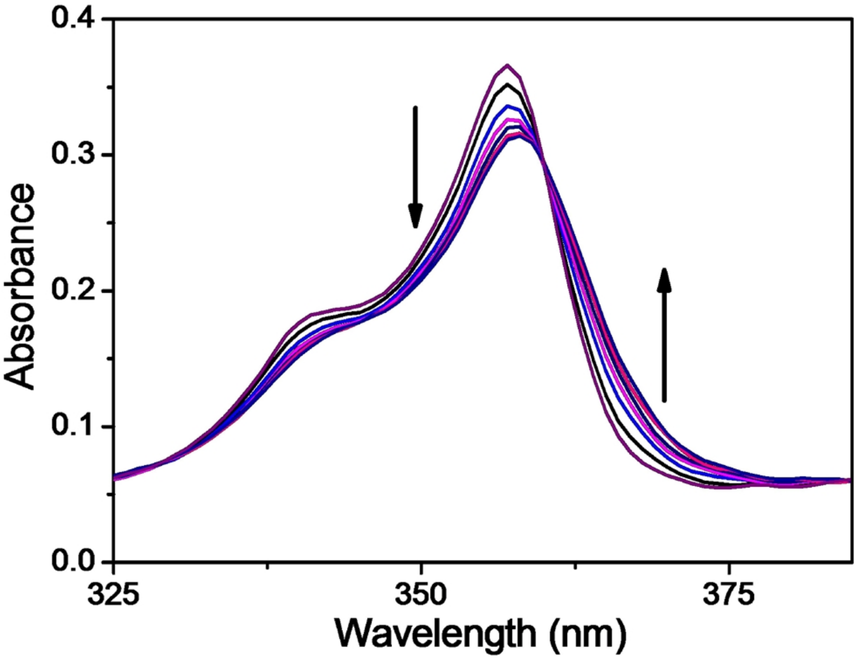

Figure S10. UV−vis spectra of 10.0 μM **G** in the presence of 0.200, 0.400, 0.600, 0.800, 1.00, and 1.20 equiv of **WP5** in water.

*6. Electrospray ionization mass spectrum of **G** with KCN*

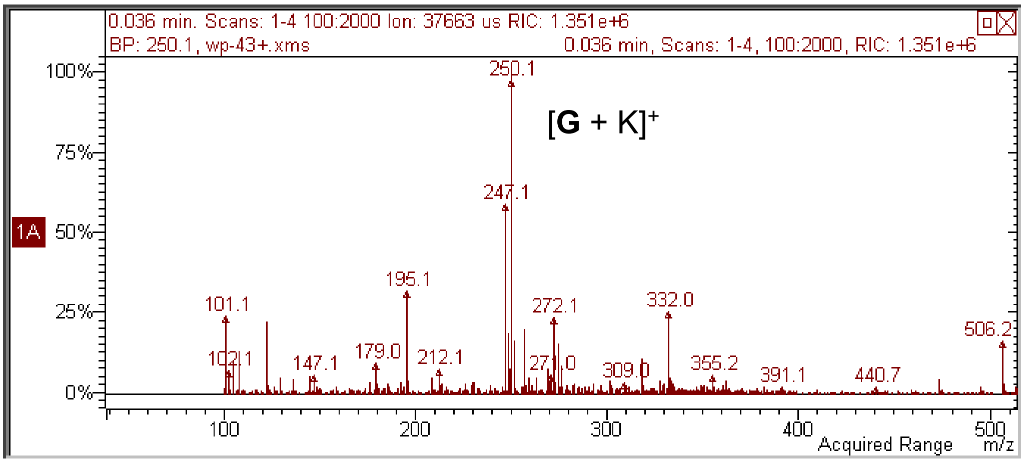

Figure S11. Electrospray ionization mass spectrum of **G** with KCN. The peak at *m*/*z* 250.1 corresponding to [**G** + K]$^+$ was clearly observed.

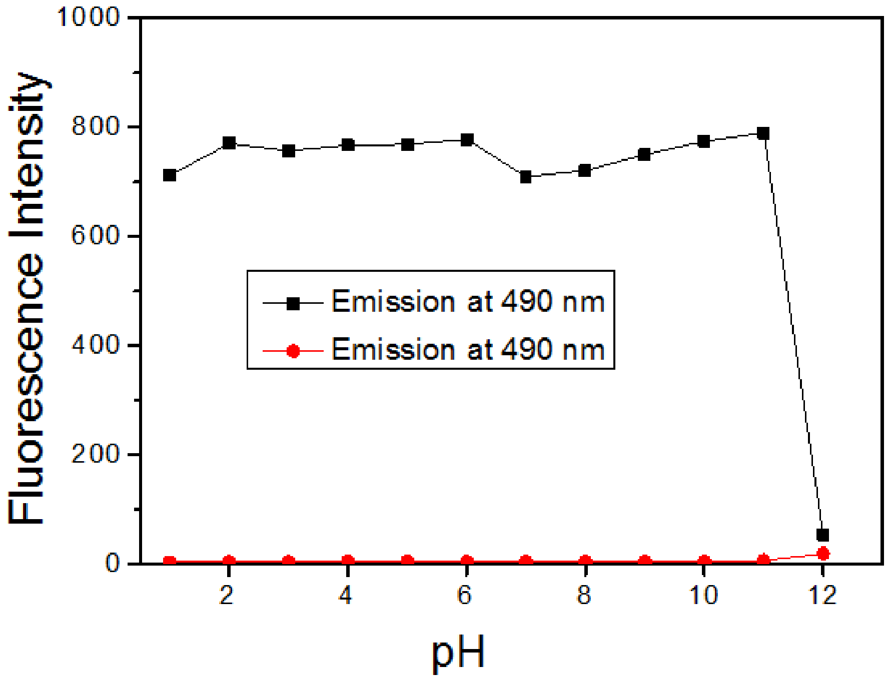

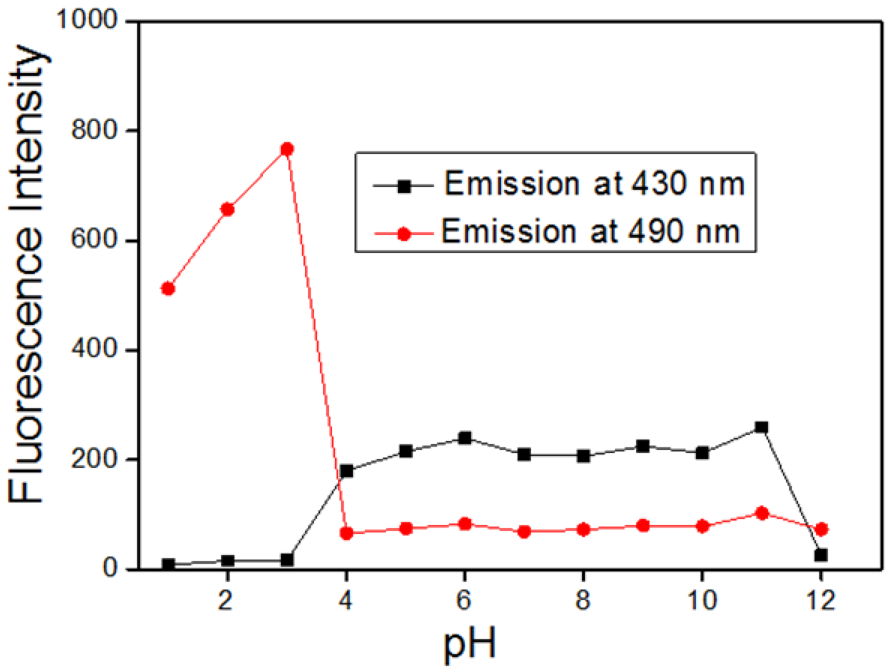

Figure S12. (Top): The fluorescence intensities at 490 nm and 430 nm for **G** (3.00 μM) at varied pH values. (Bottom): The fluorescence intensities at 490 nm and 430 nm for **G** (3.00 μM) in the presence of CN^- (20.0 equiv) at varied pH values.

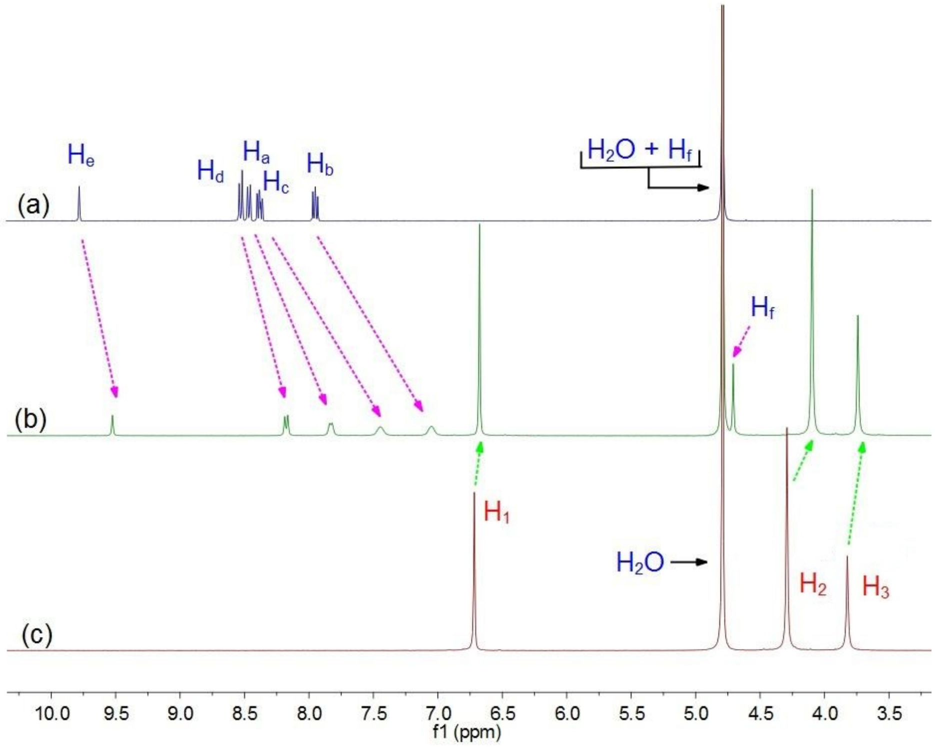

Figure 13. ^{1}H NMR spectra (400 MHz, D_2O, 298 K): (a) 10.0 mM **G**; (b) 10.0 mM **G** and **WP5**; (c) 10.0 mM **WP5**.

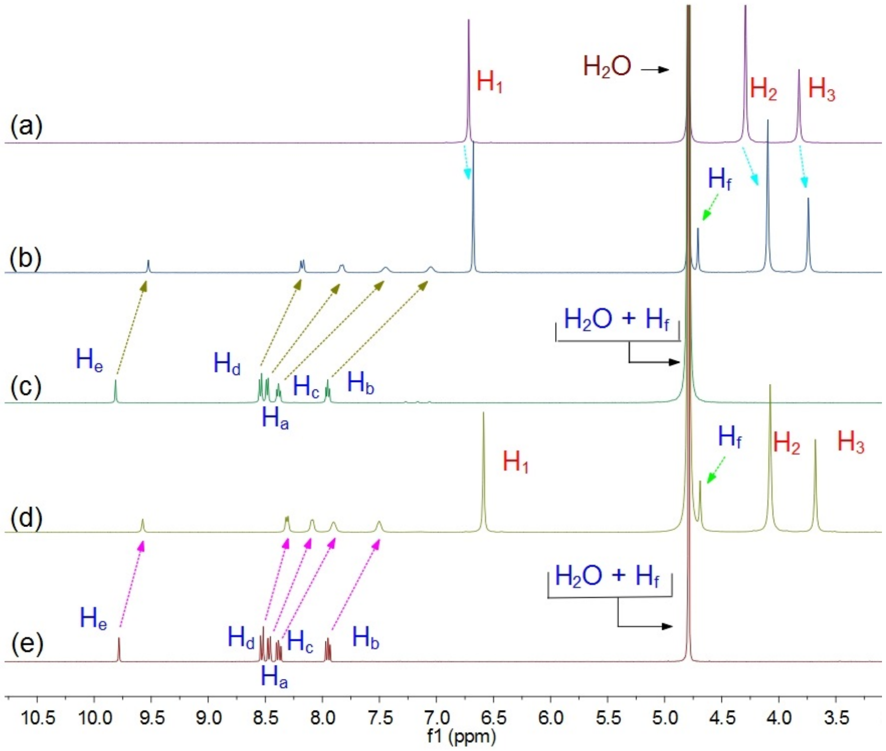

Figure S14. Partial ^{1}H NMR spectra (400 MHz, D_2O, 298 K): (a) **WP5** (10.0 mM); (b) a solution of **G** (10.0 mM) and **WP5** (10.0 mM), pH = 7.4; (c) a solution of 2.00 mL of aqueous HCl solution (37%), and 0.5 mL of **G** (10.0 mM) and **WP5** (10.0 mM), pH = 6.0; (d) a solution of 1.5 mg of NaOH, 2.00 mL of aqueous HCl solution (37%), and 0.5 mL of **G** (10.0 mM) and **WP5** (10.0 mM), pH = 7.4; (e) **G** (10.0 mM).

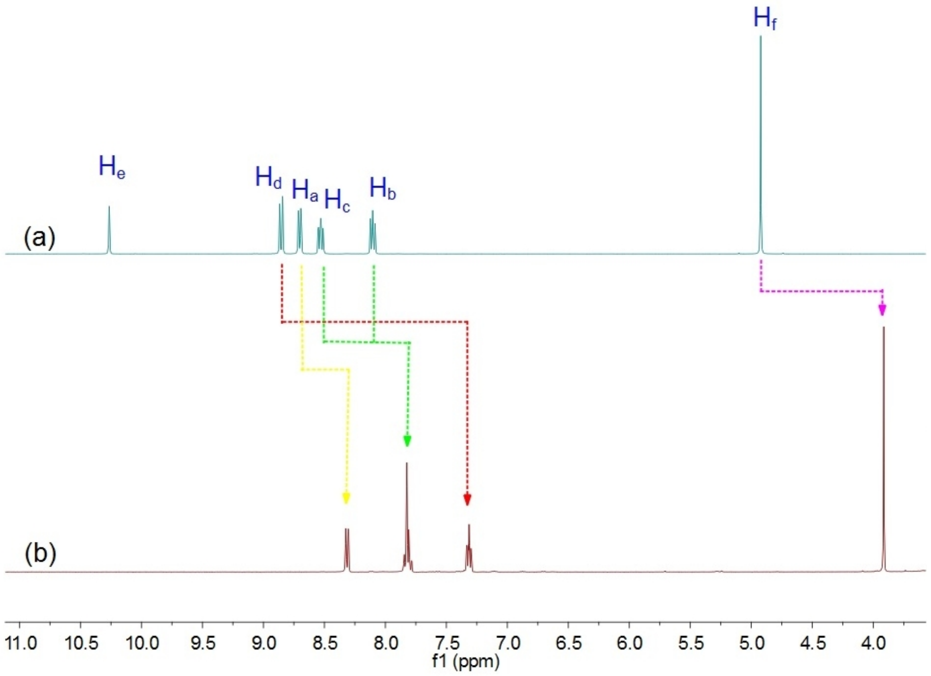

Figure S15. Partial ^{1}H NMR spectra (400 MHz, DMSO-d_6, 298 K): (a) **G** (10.0 mM); (b) **G** (10.0 mM) upon the addition of KCN (1.00 equiv).

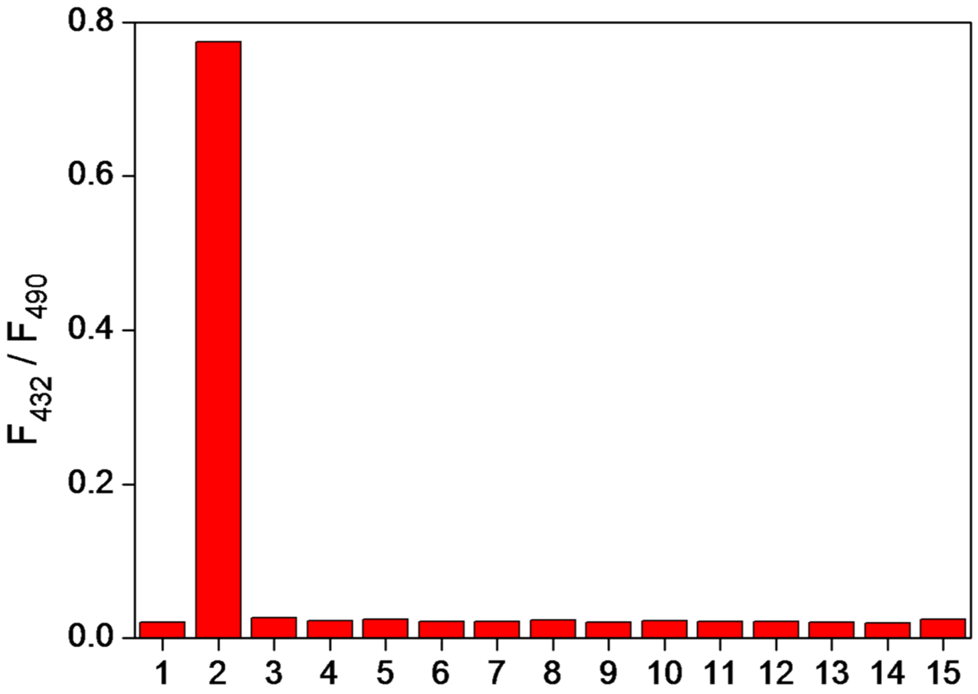

Figure S16. Fluorescence intensity ratio (F_{432} /F_{490}) of **G** (3.00 µM) upon addition of 20 equiv. of various anion specie in Tris-HCl buffer (10.0 mM, pH = 6.0). From left to right: (1) no anion (blank); (2) **G** + CN^-; (3) **G** + F^-; (4) **G** + Cl^-; (5) **G** + Br^-; (6) **G** + I^-; (7) **G** + NO_3^-; (8) **G** + HSO_4^-; (9) **G** + SCN^-; (10) **G** + AcO^-; (11) **G** + $C_6H_5CO_2^-$; (12) **G** + N_3^-; (13) **G** + CH_3S^-; (14) **G** + ClO_4^-; (15) **G** + $H_2PO_4^-$.

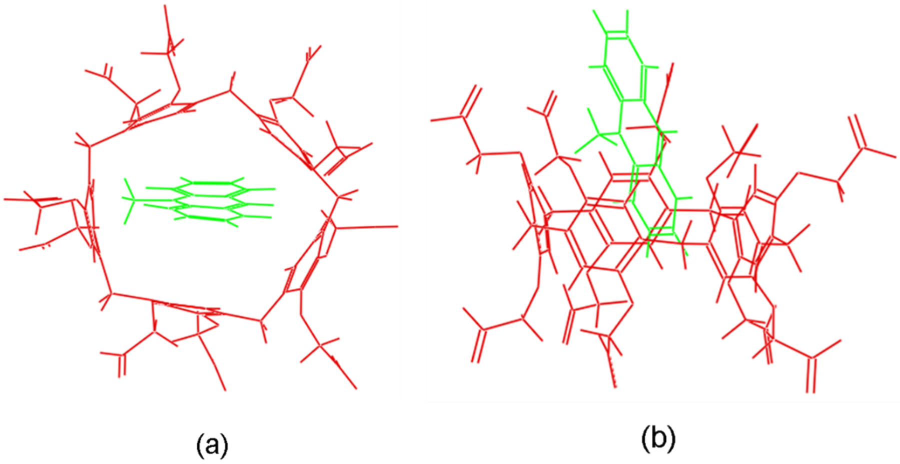

Figure S17. The energy-minimized structures of **WP5⊃G** obtained by PM6 semiempirical molecular orbital methods: (a) **WP5⊃G** (top view), (b) **WP5⊃G** (side view).

References:

S1. T. Ogoshi, M. Hashizume, T. Yamagishi and Y. Nakamoto, *Chem. Commun.*, 2010, **46**, 3708–3710.

S2 J. Joseph, E. Kuruvilla, T. Achuthan, A. D. Ramaiah and G. B. Schuster, *Bioconjugate Chem.*, 2004, **15**, 1230–1235.

S3. P. R. Ashton, R. Ballardini, V. Balzani, M. Belohradsky, M. T. Gandolfi, D. Philp, L. Prodi, F. M. Raymo, M. V. Reddington, N. Spencer, J. F. Stoddart, M.Venturi and D. J. Williams, *J. Am. Chem. Soc.*, 1996, **118**, 4931−4951.